Bioelectrochemistry 86 (2012) 9–21

Contents lists available at SciVerse ScienceDirect

Bioelectrochemistry

journal homepage: www.elsevier.com/locate/bioelechem

DNA/nickel oxide nanoparticles/osmium(III)-complex modified electrode toward selective oxidation of l-cysteine and simultaneous detection of l-cysteine and homocysteine

Ensiyeh Sharifi [a,c], Abdollah Salimi [a,b,*], Esmaeil Shams [c]

[a] Department of Chemistry, University of Kurdistan, P. O. Box 416, Sanandaj, Iran
[b] Research Center for Nanotechnology, University of Kurdistan, P. O. Box 416, Sanandaj, Iran
[c] Chemistry Department, University of Isfahan, Hezar Jarib, Isfahan, 81746–73441, Iran

ARTICLE INFO

Article history:
Received 30 September 2011
Received in revised form 25 December 2011
Accepted 31 December 2011
Available online 14 January 2012

Keywords:
DNA
NiOx nanoparticles
Osmium complex
L-cysteine
Homocysteine

ABSTRACT

The modification of glassy carbon (GC) electrode with electrodeposited nickel oxide nanoparticles (NiOxNPs) and deoxyribonucleic acid (DNA) is utilized as a new efficient platform for entrapment of osmium (III) complex. Surface morphology and electrochemical properties of the prepared nanocomposite modified electrode (GC/DNA/NiOxNPs/Os(III)-complex) were investigated by FESEM, cyclic voltammetry and electrochemical impedance spectroscopy techniques. Cyclic voltammetric results indicated the excellent electrocatalytic activity of the resulting electrode toward oxidation of l-cysteine (CySH) at reduced overpotential (0.1 V vs. Ag/AgCl). Using chronoamperometry to CySH detection, the sensitivity and detection limit of the biosensor are obtained as 44 μA mM^{-1} and 0.07 μM with a concentration range up to 1000 μM. The electrocatalytic activity of the modified electrode not only for oxidation of low molecular-mass biothiols derivatives such as, glutathione, L-cystine, L-methionine and electroactive biological species (dopamine, uric acid, glucose) is negligible but also for very similar biothiol compound (homocysteine) no recognizable response is observed at the applied potential window. Furthermore, the simultaneous voltammetric determination of L-cysteine and homocysteine compounds without any separation or pretreatment process was reported for the first time in this work. Finally, the applicability of sensor for the analysis of CySH concentration in complex serum samples was successfully demonstrated. Highly selectivity, excellent electrocatalytic activity and stability, remarkable antifouling property toward thiols and their oxidation products, as well as the ability for simultaneous detection of L-cysteine and homocysteine are remarkably advantageous of the proposed DNA based biosensor.

1. Introduction

Sulfur-containing amino acids, such as homocysteine (HCySH) and L-cysteine (CySH) play crucial roles in biological systems for the diagnosis of disease states [1,2]. CySH is known as an active site in the catalytic function of certain enzymes called cysteine proteases [3] and its deficiency is involved in slowed growth, hair depigmentation, edema, lethargy, liver damage, muscle and fat loss, skin lesions, and weakness [4]. It is also widely used in the food industry as an antioxidant and in the pharmaceutical industry in drug formulation [5]. An elevation in the concentration of total plasma HCySH is known as an independent risk factor for the development of cardiovascular and Alzheimer's disease [6]. Furthermore, alterations in HCySH metabolism have also been observed clinically in diabetic patients [7-9]. Therefore, the rapid, sensitive and selective detection of HCySH and CysH are very important for investigating their functions in cells and disease diagnosis [6,10-14].

Numerous methods for the determination of thiols have been reported so far. Most of them are based on the chromatographic separation [15,16], electrophoretic methods [17,18], spectrometric methods [19,20], colorimetric and fluorimetric detection [11,12,14]. Separation methods present basic limitations in terms of equipment cost, complexity, sample processing and run times. Furthermore, simultaneous detection of CySH and HCySH with colorimetric and fluorimetric methods without a separation technique is impossible. Among different methodologies used, electrochemical measurements of thiols have attracted considerable interest because of their high sensitivity, simplicity, low cost and feasibility to the development in vivo sensors and chromatographic detectors [21-26]. Although significant advancement has been made on the electrochemical methods, sensors capable of selective detection of CySH are rather few. In addition, some reported electrodes suffer from certain drawbacks, such as instability [22,24], large overpotential [27,28] and low sensitivity [26] which reduces detection selectivity, especially in the case of biological and real samples. Thus, the development of an electrochemical

* Corresponding author at: Department of Chemistry, University of Kurdistan, P. O. Box 416, Sanandaj, Iran. Tel.: +98 871 6624001; fax: +98 871 6624008.
E-mail addresses: absalimi@yahoo.com, absalimi@uok.ac.ir (A. Salimi).

1567-5394/$ – see front matter © 2012 Elsevier B.V. All rights reserved.
doi:10.1016/j.bioelechem.2011.12.013

method for sensitive and selective determination of CySH is now much in demand. On the other hand, few papers offer procedures for simultaneous quantification of CySH and HCySH [29,30] and the electrochemical methods that have been designed to detect these biothiols are used in conjunction with chromatographic methods [31-33]. To the best of our knowledge, there is only one report on simultaneous direct electrochemical detection of CySH and HCySH [34]. However, low sensitivity and overlapping of CySH and HCySH signals are mainly disadvantageous of the sensor. Therefore, the design of suitable modified electrode that can be able to simultaneously detect these important biothiol compounds, without the assistance of separation techniques, is highly demanding, particularly for the analysis of biological samples.

Today, with the development of nanoscience and nanotechnology, there have been various trials to employ new nanomaterials in fabricating chemically modified electrodes. Among different nanomaterials, nickel oxide (NiOx) nanoparticles have received considerable attention in recent years due to their catalytic, optical, electronic and magnetic properties [35,36]. Because of their easy preparation process, electroinactivity in physiological pH solutions and high porosity, NiOx nanoparticles have been widely investigated and applied to immobilize different biomolecules and enzymes as well as fabrication of sensors and biosensors [37-39].

Deoxyribonucleic acid (DNA) as an important biological macromolecule has been paid much attention in the recent years. It is not only due to the intriguing genetic information of the molecule, but also DNA is conductive polymer which conducts electrons well due to its double helical structure. The base pairs stacked within double helical DNA can provide an effective medium for electron transfer [40-42], so it could be used as an ideal platform for fabrication of electrochemical sensors. Because of the biological importance of DNA, metal oxide nanoparticles/DNA conjugates have been developed to provide unique functions for various studies such as designing DNA hybridization sensors and evaluating photoinduced DNA damage [43,44]. In addition, hybrid materials formed by the combination of nanoparticles and DNA have been demonstrated as an efficient way to produce nanostructured materials that can respond to a specific stimulus with a particular signal [45,46]. The application of thionine/DNA/nano-TiO_2 modified electrode has been reported for detection of H_2O_2 [47]. DNA molecules also have been used as a template for fabricating and assembling the different hybrid nanomaterials [48]. Zu and coworkers have reported a method for the growth of oxidized nickel nanoparticles on a DNA template in aqueous solution [49].

In the present study, an electrochemical method is used for the fabrication of a NiOx nanoparticle/DNA nanobiocomposite on the surface of glassy carbon electrode. This modified electrode is applied as an ideal platform for entrapment of osmium complex as an excellent electron transfer mediator. The electrocatalytic activity of the GC/DNA/NiOxNPs/Os(III)-complex modified electrode has been investigated toward oxidation of CySH. Due to the excellent electrocatalytic ability of Os (IV)/Os (III) redox couple and the unique physiochemical properties of DNA/NiOx nanobiocomposite, the overpotential for CySH oxidation significantly reduced and thus, the mentioned biosensor can be used for highly selective and sensitive detection of CySH. Moreover, based on the interaction of CySH and HCySH with DNA/NiOx/Os(III)-complex nanobiocomposite, well-separated voltammetric signals were observed for these biomolecules. Simultaneous determination of CySH and HCySH without further pretreatment or separation process has been realized.

2. Experimental

2.1. Materials

Double stranded DNA (from calf thymus) produced by Sigma, and it is used as received without further purification. Osmium(III)-complex;1,4,8,12 tetraazacyclotetradecane osmium(III) chloride, $(Os(III)LCl_2)$ ClO_4 is synthesized and purified based on the reported procedure [50]. CySH, HCySH and Cystine are obtained from Sigma. L-Methionine, thiocytosine, glutathione, oxalic acid, dopamine , uric acid and other chemicals are obtained from Fluka. The $Ni(Cl)_2$ and all other chemicals were of analytical grade from Merck and used without further purification. The buffer solutions (0.1 M) at pH range 2–12 were prepared from H_3PO_4, CH_3COOH, NaH_2PO_4 and Na2HPO4, and HCl and NaOH solutions were used for pH adjustment. All solutions are prepared in double distilled water and are deaerated with high purity nitrogen prior to the experiments.

2.2. Apparatus and procedures

All electrochemical measurements are carried out with a three-electrode system comprising modified and unmodified glassy carbon as working electrode, an Ag/AgCl (3 M KCl) as reference and a platinum wire as auxiliary electrode. Surface morphology is examined using Vega-Tesacn electron microscope (SEM). Amperograms are carried out with a Metrohm multi-purpose instrument model 693VA Processor, equipped with a 694VA Stand. Cyclic voltammograms are performed with a computer controlled μ-Autolab modular electrochemical system (Eco Chemie Ultrecht, The Netherlands), driven with GPES software (Eco Chemie). All measurements are done at room temperature (25 °C). The Zview impedance software (version 2.3f) is used for data fitting.

2.3. Preparation of GC/DNA/NiOx/Os(III)-complex modified electrode

The GC electrode (2 mm diameter) is carefully polished with alumina, and then ultrasonicated in ethanol and double distilled water, respectively to remove adsorbed particles. Electrodeposition of DNA on the surface of GC electrode is processed according to the procedure reported by Lin and his coworkers [51]. In summary, the GC electrode is immersed in 0.1 mg/ml DNA solution (PBS). The electrodeposition of DNA molecules onto the GC electrode is performed by keeping the electrode potential at 1.7 V (*vs.* Ag/AgCl) for 30 min. Then, the GC electrode is rinsed with double distilled water to remove any physically absorbed DNA. Afterwards, DNA modified GC electrode is immersed in acetate buffer solution (pH 6) containing 1 mM nickel chloride in order to have electrostatic adsorption of Ni^{2+} onto DNA networks. Then, the electrode is immersed in PBS (pH 11) and the potential is repetitively cycled (20 scans) between 0.0 and 0.6 V at a scan rate of 0.05 Vs^{-1} for electrodissolution and passivation of NiOx nanoparticles on the surface of GC electrode modified with immobilized DNA layer [52]. Finally, 20 μL of 0.1 mM Os (III)-complex solution in acetonitrile is dropped on the surface of GC/DNA/NiOx electrode and dried in air. The modified electrode is washed with double distilled water and stored in PBS (pH 7) at refrigerator (4 °C) before using in experiments. The same procedure was used for the construction of GC/DNA/Os(III)-complex and GC/NiOx/Os(III)-complex electrodes in the absence of nickel ions and DNA, respectively. The GC/NiOx electrode is manufactured as reported previously by our group [38].

2.4. Real sample preparation

For the determination of total CySH, 200 μL of a freshly prepared 2.5 M $NaBH_4$ solution was added to the 200 μL of serum sample. After being mixed, the solution was incubated in a 50 °C water bath for 30 min under gentle stirring to reduce the disulfide bonds. After cooling to room temperature, an aliquot of 3 M $HClO_4$ was added in order to decompose excess $NaBH_4$. The mixture then centrifuged at 3000 rpm for 10 min and the supernatant was collected. The reduced mixture was centrifuged at 3000 rpm for 20 min and the supernatant was collected.

3. Results and discussions

3.1. Electrode characterization

The NiOx nanoparticles deposited on the GC and GC/DNA electrodes are characterized using scanning electron microscopy (SEM) and cyclic voltammetry techniques. As shown in (Fig. 1A), the NiOx nanoparticles were uniformly distributed on all locations of the GC/DNA electrode surface and the size of NiOx nanoparticles varies from 50 to less than 100 nm. While the morphology of GC electrode modified with NiOx nanoparticles is different (Fig. 1B), it confirms that the DNA plays an important role in distributing of nanoparticles evenly on the surface of electrode. The particle size for electrodeposited NiOx nanoparticles onto bare GC electrode varied between 20 and 50 nm. The entrapment of nickel oxide layer on the DNA networks was also investigated by recording cyclic voltammograms of modified electrode in alkaline solution (Fig. 1 supplement). As illustrated, the anodic peak at 0.47 V is observed due to the oxidation of the $Ni(OH)_2$ phase to NiO(OH). The corresponding cathodic peak at 0.405 V represents the reduction of NiO(OH) to $Ni(OH)_2$ [52]. Increase of the anodic peak current during consequent potential cycling in the solution free of Ni^{2+} indicates electrodissolution and passivation of nickel oxide nanoparticles on the surface of GC/DNA electrode.

3.2. Electrochemical behavior of GC/DNA/NiOxNPs/Os(III)-complex electrode

The electrochemical properties of Os(III)-complex in acetonitrile solution and Os(III)-complex/CNTs modified GC electrodes at various pHs have been studied previously [53]. In the current work, the electrochemical behavior of Os(III)-complex is investigated on the surface of GC/DNA/NiOx nanocomposite modified electrode. Fig. 2 shows the cyclic voltammograms of the Os(III)-complex immobilized onto GC/NiOx (a), GC/DNA (b) and GC/DNA-NiOxNPs (c) modified electrodes in 0.1 M PBS (pH 7). The cyclic voltammograms clearly illustrate a redox couple attributed to the Os(IV)/Os (III) redox center ($E^0 = 0.1$ V). It is obvious that the GC/DNA/NiOx/Os(III)-complex modified electrode exhibits a well-shaped peak with higher current density compared to both electrodes of GC/DNA/Os(III)-complex and GC/NiOx/Os(III)-complex. These results clearly indicate the high loading ability of DNA/NiOx nanocomposite for Os (III)-complex and thus, the DNA/NiOx nanocomposite modified electrode is quite suitable for adsorption of Os(III)-complex. The magnitude of peak current for Os(III)-complex immobilized onto DNA/NiOx nanocomposite (c) is five and four times higher than on a GC/DNA (a) and GC/NiOx (b) modified electrodes, respectively; which further confirms the efficiency of DNA/NiOx modified electrode. The same voltammetric behavior has been observed for redox compounds adsorbed onto DNA/nano-TiO_2 bilayer [47]. Also for GC electrode modified with Os(III)-complex, no recognizable redox response was observed at the same experimental condition.

Fig. 3 shows the Nyquist plots of GC electrode (a), GC/DNA (b), GC/DNA/NiOx (c) and GC/DNA/NiOxNPs/Os(III)-complex (d) modified electrodes in 0.1 M KCl solution containing 2.5 mM $[Fe(CN)_6]^{3-/4}$ at frequency range of 0.1 Hz to 100 kHz. The straight line at low frequency is related to the diffusion process known as Warburg element, while the high frequency semicircle is related to the electron transfer resistance. As can be seen for bare GC electrode, a very small semicircle ($R_{ct} = 250\ \Omega$) is found due to very low electron transfer resistance to the redox probe. After immobilization of DNA, the value of R_{ct} is significantly increased to about 9500 Ω. It indicates hindrance to the electron transfer, confirming the successful immobilization of DNA onto GC electrode surface. After modification of GC electrode with DNA and NiOx, the electron transfer resistance (R_{ct}) decreased to 5800 Ω, which proved that the assembly of NiOx makes the electron transfer easier. With further immobilization of GC/DNA/NiOx with Os(III)-complex, the R_{ct} decreased to 4000 Ω, due to the decrease in the surface negative charge. Therefore, adsorption of Os(III)-complex onto the DNA/NiOx nanocomposite facilitates the electron transfer of the redox probe on the modified electrode. These data show that DNA/NiOxNPs/Os(III)-complex are successfully attached to the GC surface.

The stability of the modified electrode is checked by recording successive sweeps of cyclic voltammograms in 0.1 M PBS (pH 7) (not shown). The GC electrode modified with DNA/NiOxNPs/Os(III)-complex displayed stable and reproducible electrochemical behavior

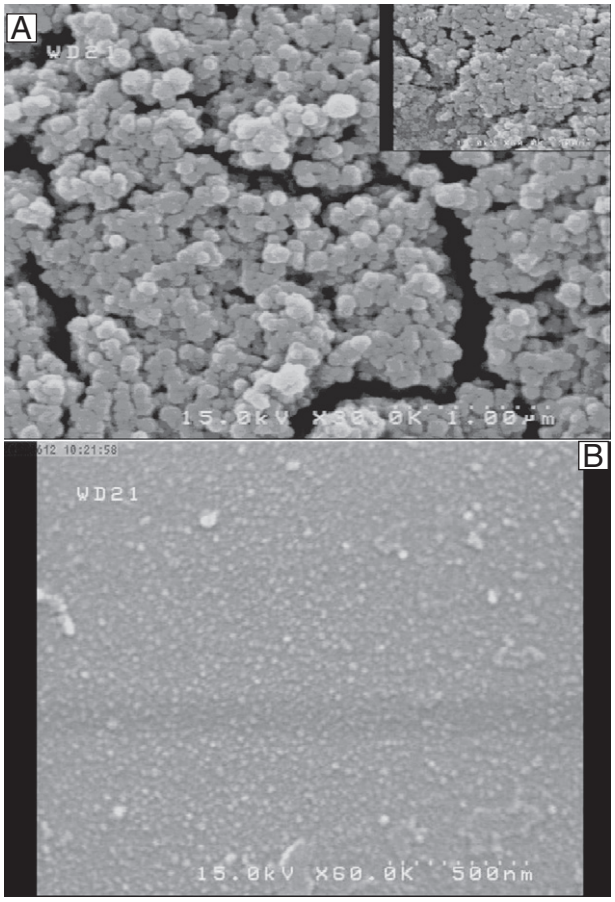

Fig. 1. (A) SEM image of the NiOx nanoparticles deposited onto GC/DNA modified electrode. (B) SEM image of the electrodeposited NiOx nanoparticles on bare glassy carbon electrode.

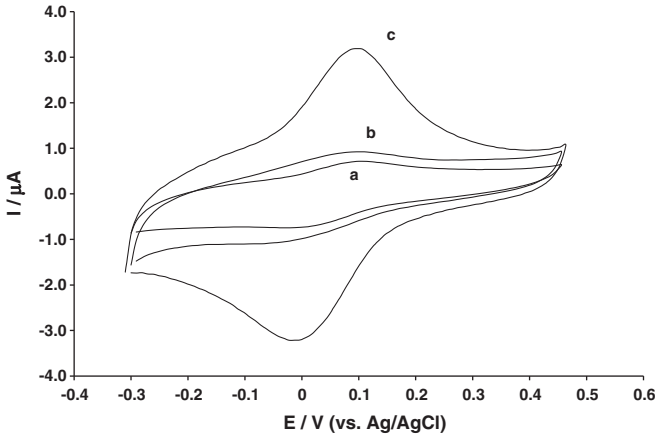

Fig. 2. Cyclic voltammograms of GC/NiOxNPs/Os(III)-complex (a), GC/DNA/Os(III)-complex (b) and GC/DNA/NiOxNPs/Os(III)-complex (c) modified electrodes in 0.1 M PBS (pH 7), scan rate 100 mV s^{-1}.

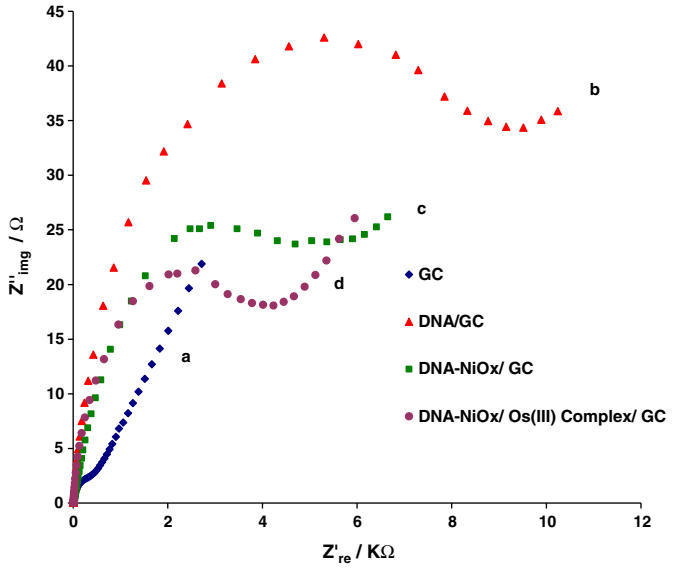

Fig. 3. (A) Nyquist plots for different modified electrodes in 0.1 M KCl solutions containing 2.5 mM of $K_3Fe(CN)_6 + K_4Fe(CN)_6$ and at applied potential of 0.15 V and frequency range from 0.1 to 10^5 Hz.

and no appreciable changes (less than 3%) observed either in the peak current or the peak potential values after 220 consequent cycles. Furthermore, the current response of the modified electrode is decreased by only 3% when the electrode is immersed in PBS (pH 7) for 24 h. In contrast to GC/DNA/NiOxNPs/Os(III)-complex modified electrode, redox peak currents of GC/DNA/Os(III)-complex and GC/NiOxNPs/Os(III)-complex are continuously decreased and completely disappeared after 30 cycles or when immersing in PBS (pH 7) for 2 h. These results further represent the excellent stability of nanobiocomposite bilayer for immobilization of Os(III)-complex. The reproducibility of the fabrication method is also evaluated by preparing five electrodes and recording their cyclic voltammograms. The relative standard deviation of 4% is observed for anodic peaks measurement of prepared modified electrodes.

Cyclic voltammograms of the modified electrode at different scan rates in potential range of −0.3 to 0.45 V in 0.1 M PBS (pH 7) were recorded (Fig. 2 supplement). By measuring the variation of peak potential versus log of scan rate and based on Laviron theory [54], the electron transfer coefficient (α) and electron transfer rate constant (k_s) for GC/DNA/NiOxNPs/Os(III)-complex modified electrode were calculated as 0.45 and 2.3 s^{-1}, respectively. The effect of the pH on the electrochemical behavior of Os(III)-complex immobilized onto GC/DNA/NiOx modified electrode is studied in different buffer solutions (pH 2–12). The pH dependence of the formal electrode potentials from pH 2 to 12 is obtained as follows:

$$E^{0'}/\mathrm{mV} = -62.1(\pm 3)\mathrm{pH} + 487(\pm 18)\left(R^2 = 0.9988\right) \quad (1)$$

This slope is close to the theoretical value of −59.1 mV pH^{-1} at 25 °C. So the electrode kinetics involves a rate determining electron-transfer step preceded by a reversible deprotonation step and it well agrees with the results observed for Os(III)-complex immobilized on the surface of SWCNTs modified GC electrode [53].

3.3. Electrocatalytic oxidation of L-cysteine at GC/DNA/NiOxNPs/Os(III)-complex modified electrode

Due to high reversibility and excellent electrochemical stability of GC/DNA/NiOxNPs/Os(III)-complex modified electrode, its electrocatalytic activity toward CySH oxidation is investigated. The oxidation of CySH at GC/DNA/NiOxNPs and GC/DNA/NiOxNPs/Os(III)-complex electrodes is investigated in PBS (pH 7). Fig. 4 shows recorded cyclic voltammograms in the absence and presence of 2 mM of CySH at GC/DNA/NiOxNPs and GC/DNA/NiOxNPs/Os(III)-complex electrodes at scan rate of 20 mV s^{-1}. As can be seen, no electrochemical response at GC/DNA/NiOxNPs electrode is observed in the absence of CySH (voltammogram "a"), but in the presence of CySH a small redox response can be seen (voltammogram "b"). However, in the same conditions at GC/DNA/NiOxNPs/Os(III)-complex electrode, the oxidation current of CySH starts at −0.15 V and an obvious catalytic oxidation peak appears at the potential of 0.1 V(voltammogram "d"). It can be seen that peak potential for oxidation of CySH is significantly shifted to a more negative potential (0.1 V vs. Ag/AgCl) compared to the GC/DNA/NiOxNPs modified electrode (0.6 V *vs.* Ag/AgCl). Furthermore, the anodic peak current is greatly enhanced in the presence of CySH and the reduction peak current totally disappeared, suggesting a typical electrocatalytic oxidation process. The substantially decreasing overvoltage and increasing oxidation peak current of CySH confirm that Os(III)-complex immobilized onto GC/DNA/NiOx electrode can act as an efficient mediator to shuttle electrons between CySH and working electrode and facilitate electrochemical regeneration following electron exchange with CySH.

To understand the undergoing electrochemical reactions at the different modified electrodes, the EIS experiments are performed in the presence of 0.1 mM of CySH. The complex plane plots and equivalent circuit are shown in Fig. 5 As can be seen for GC electrode, a semicircle curve is observed over the whole frequency region, indicating that the reaction is kinetically controlled. Equivalent circuit analysis shows charge transfer resistance (R_{ct}) of 3.2 MΩ, $C_{dl} = 0.366$ μF and $n = 0.926$. In the equivalent circuit, R_{ct}, R_s and C_{dl} represent the faradic charge transfer resistance, bulk resistance of solution and double layer capacitance, respectively. The n indicates the deviation of C_{dl} from pure capacitance. For GC/DNA, GC/DNA/NiOxNPs and GC/DNA/NiOxNPs/Os(III)-complex, the calculated charge transfer resistance is dropped to 0.38, 0.232 and 0.100 MΩ, respectively. The results indicate that the immobilized DNA increases the charge transfer kinetics to about one-ninth of that at the bare GC electrode. The anionic phosphate backbone of DNA adsorbs the proton of thiols group in CySH molecule, which accelerates the electrooxidation processes. The same results were observed for oxidation of other protonated molecules such as tripropylamine (TPA) in the presence of DNA molecules [55]. The C_{dl} and n for GC/DNA, GC/DNA/NiOxNPs and GC/DNA/NiOxNPs/Os(III)-complex were 0.326 μF and 0.898, 0.745 μF and 0.925 and 0.463 μF and 0.912, respectively. For GC electrode modified with DNA/NiOx nanocomposite, the charge transfer resistance is decreased up to 150 kΩ compared to electrode

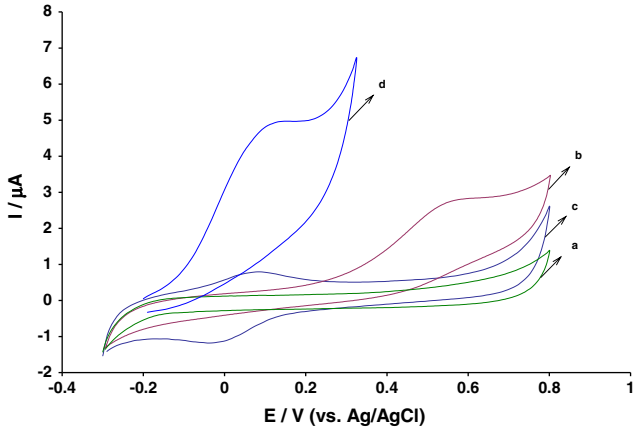

Fig. 4. Recorded cyclic voltammograms of GC/DNA/NiOxNPs electrode in the absence (a) and presence of 2 mM CySH(b); (c) and (d) as (a) and (b) for GC/DNA/NiOxNPs/Os(III)-complex modified electrode at scan rate of 20 mV s^{-1} and in 0.1 M PBS (pH 7).

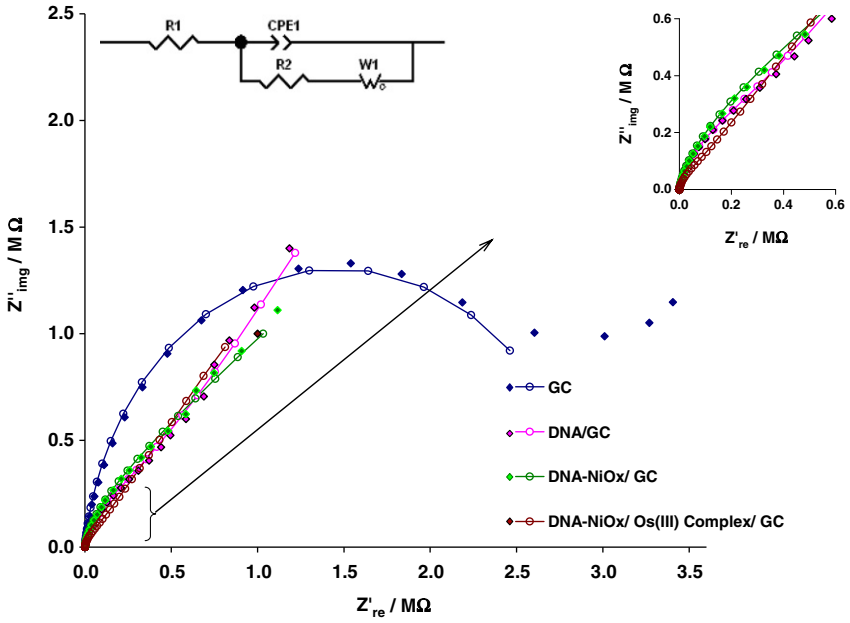

Fig. 5. Nyquist plots (fitted and experimental data) of GC, GC/DNA, GC/DNA/NiOxNPs and GC/DNA/NiOxNPs/Os(III)-complex electrode in 0.1 M PBS (pH 7) containing 0.1 mM CySH. EIS conditions: initial potential, 0.15 V; amplitude voltage, 5 mV; frequency range, 100 kHz to 0.1 Hz. Inset: Equivalent circuit used to model impedance data in the presence of redox couples.

modified with DNA, which proves that the assembly of NiOx nanoparticles and DNA makes the electron transfer easier. After immobilization of Os(III)-complex onto GC/DNA/NiOxNPs modified electrode, the charge transfer resistance is decreased to 100 kΩ. Thus, the Os(III)-complex film clearly plays an essential role in increasing the electron transfer kinetics of CySH oxidation at the surface of modified electrode. The adsorption of Os(III)-complex on DNA/NiOx nanocomposite facilitated the electron transfer of the electrochemical probe on the modified electrode.

For further investigating the electrocatalytic properties of different modified electrodes containing DNA, NiOx, Os(III)-complex and their various combinations, cyclic voltammograms of these electrodes in the presence of CySH at a wide potential range were recorded. Cyclic voltammograms of GC (a), GC/NiOxNPs (b), GC/DNA (c), GC/DNA/NiOxNPS (d) and GC/DNA/NiOxNPs/Os(III)-complex (e) modified electrodes in the presence of CySH were shown (Fig. 3 supplement). As can be seen, the electrocatalytic current response of GC/NiOxNPs (b), GC/DNA (c) and GC/DNA/NiOxNPs (d) modified electrodes at 0.57 V is 1.2, 1.7 and 2.1 μA, respectively, which is in agreement with EIS data for charge transfer kinetics on the different modified electrodes. Compared to the GC/NiOxNPs, GC/DNA and GC/DNA/NiOxNPs modified electrodes, the GC/DNA/NiOxNPs/Os(III)-complex electrode exhibits a well-shaped peak and largest catalytic current for the oxidation of CySH in less positive potential (0.10 V *vs.* Ag/AgCl). It has also been found that the oxidation of CySH is started from −0.15 V and well-defined peak is observed at 0.1 V (peak I). Moreover, the second peak for oxidation of CySH appeared at 0.570 V (peak II). This means the oxidation of CySH at GC/DNA/NiOxNPs/Os(III)-complex electrode

Table 1
Analytical characteristics of different cysteine electrochemical sensors.

Electrode	E_p/V (vs. Ag/AgCl)	LOD (μM)	Sensitivity μA/mM	Linear range (μM)
Electrospun carbon nanofibers modified CPE [28]	0.7 (pH 7)	0.1	0.0159	0.15–63.8
Poly N,N-dimethylaniline /ferrocyanide film/CPE [67]	0.15 (pH 6)	6.38	–	7.40 -138
Ordered mesoporous carbon [68]	0.47 (pH 7)	0.1	18	3–130
Boron-doped carbon nanotube /GCE [69]	0.50 (pH 7)	0.26	0.0253	0.78-200
β-MnO2 Nanowires/ chitosan/GCE [61]	0.5 (pH 7.8)	0.07	–	0.5–630
Oxo-guanine/ZnO nanoparticle/GCE [70]	0.5 (pH 7)	0.05	0.0285	0.3-20
Copper-cobalt hexacyanoferrate/CPE [71]	0.74 (pH 7)	5	–	6-1000
Poly-3,4-hylenedioxythiophene/screen-printed electrode [72]	0.586(pH 6)	0.03	52.7	0.05–200
Carbon ionic liquid electrode [60]	0.49 (pH 7)	1	–	2-210
Fl Fluorosurfactant-modified gold electrode [41]	0.25 (pH 7)	0.5	2.57	Up to 200
Poly(diallyldimethylammonium chloride/MWCNTs)/GCE [73]	0.7 (pH 7)	0.3	13.8 nA/M	20-1300
MWCNTs-modified GCE [74]	0.27 (pH 4)	5.4	3.0	10-500
Platinum /CNTs electrode [75]	0.48(pH 7.4)	0.3	–	0.5–1000
Ru[(tpy)(bpy)Cl]PF6/sol–gel CCE [76]	0.8 (pH 2)	1	5.0	5–685
Cobalt(II) salophen-modified CPE [27]	0.6 (pH 7)	2	–	2–10000
Lead ruthenate pyrochlore modified electrode [77]	0.5 (pH 7.4)	2.91	32	Up to 560
GC/DNA-NiOxNPs/Os(III)-complex electrode (present study)	0.10 (pH 7)	0.07	44	1–1000
	0.0 (pH 7)	0.27	23	3–400

CPE: Carbon paste Electrode; G CE: Glassy carbon electrode; CCE:Carbon ceramic electrode; CNTs: Carbon nanotubes; MWCNTs: Multi walled carbon nanotubes.

undergoes two processes, and the Os(III)-complex film clearly plays an essential role in the observed electrocatalytic oxidation of CySH in low overvoltage (peak I), illustrating that peak I is attributed to the electrocatalytic oxidation of CySH by Os(III)-complex. The high conductivity of DNA/NiOxNPs/Os(III)-complex nanocomposite film increases the electrical properties of the redox processes as well as available surface area. While peak II at the modified electrode is at the same potential as that at the GC/NiOx electrode, which means peak II could be logically corresponded to the oxidation of CySH at uncovered sites of modified electrode with Os (III)-complex. No cathodic peak is observed on the reverse scan within the investigated potential range (0 to +0.65 V) because CySH oxidation is an electrochemically irreversible process. The electrochemical oxidation of CySH for peak I occurred by the possible mechanisms at the modified electrode proposed as follows:

$$CySH \leftrightarrows CyS^- + H^+ \quad (2)$$

$$Os(III) - complex \rightleftarrows Os(IV)^+ - complex + e^- \quad (3)$$

$$CyS^- + Os(IV)^+ - complex \rightarrow CyS^{\bullet} + O(III) - complex \quad (4)$$

$$2\ CyS^{\bullet} \rightarrow CySSCy \quad (5)$$

This is similar to the mechanism reported previously for CySH oxidation on solid electrodes [56]. For peak II, the following mechanism describes the electrooxidation of CySH [57].

$$CySH \rightleftarrows CyS^- + H^+ \quad (6)$$

$$CyS^- \rightarrow CyS^{\cdot} + e^- \quad (7)$$

$$2\ CyS^{\bullet} \rightarrow CySSCy \quad (8)$$

Considering selectivity of the modified electrode for determination of CySH and also antifouling properties of the modified electrode in low overpotential, the first peak of CySH oxidation at +0.10 V vs. Ag/AgCl, is chosen for analytical determination of CySH. Compared to many of the substrates reported previously, GC/DNA/NiOxNPs/Os(III)-complex electrode exhibits significantly low overpotential for the oxidation of CySH (Table 1), indicating significant catalytic ability of GC/DNA-NiOxNPs/Os(III)-complex electrode for CySH oxidation. Fig. 6 [A] illustrates cyclic voltammograms of the modified electrode in 0.1 M PBS (pH 7), containing various concentrations of CySH

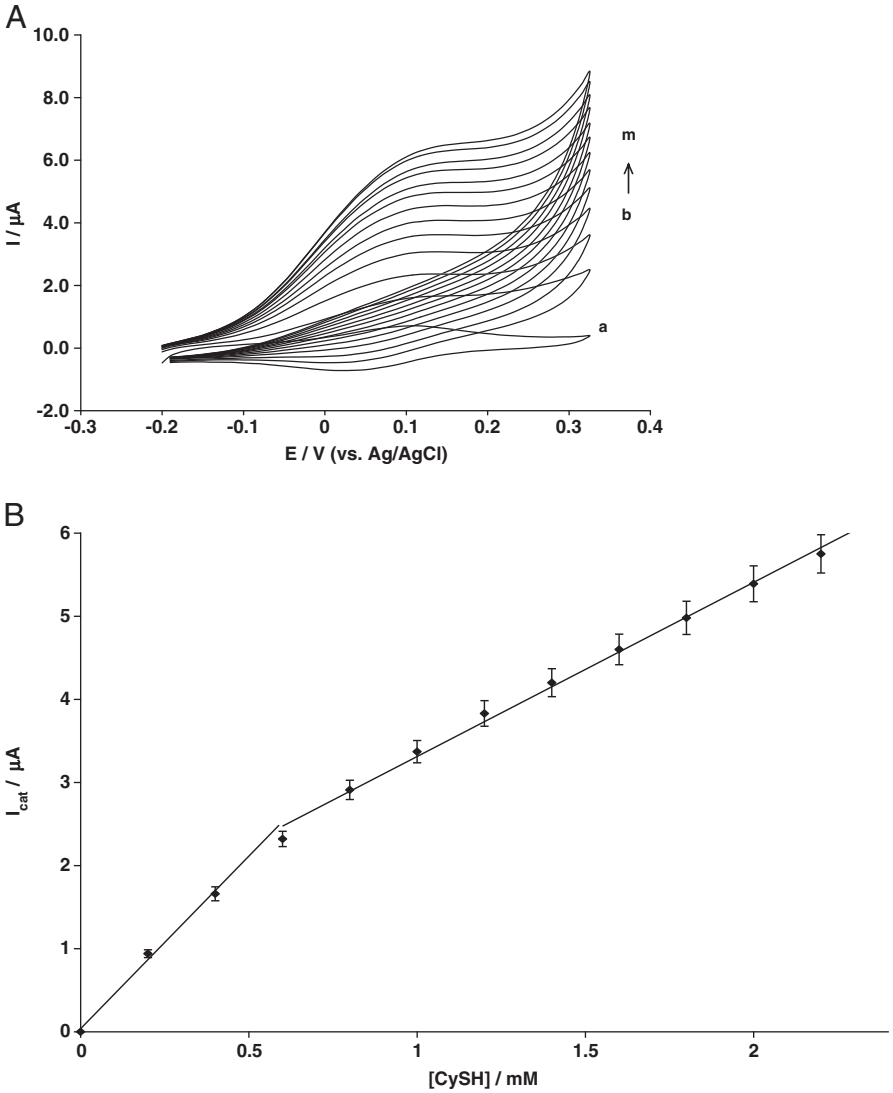

Fig. 6. (A): Cyclic voltammograms of GC/DNA/NiOxNPs/Os(III)-complex modified electrode in 0.1 M PBS (pH 7) at scan rate of 20 mV s^{-1} (a) in the absence of CySH and (b to m) in the presence of different concentration of CySH (from inner to outer 0.2–2.4 mM). (B): Plot of catalytic peak current I_p/µA *vs.* concentration of cysteine [CySH/mM].

(0.5–3.5 mM). The calibration plots of catalytic current vs. CySH concentration are shown in Fig. 6 [B]. As is obvious, the catalytic peak current of the modified electrode increases linearly with increasing CySH concentration in two concentration ranges, one from 0 to 0.6 mM with the regression equation of $I/\mu A = 4.15\ (\pm\ 0.08)$ [CySH]/mM + 0.037 ($\pm$ 0.002)/ μA ($R^2 = 0.9942$) and another from 0.6 to 2.4 mM with the regression equation of $I/\mu A = 2.0958\ (\pm\ 0.15)$ [CySH]/mM + 1.2158 ($\pm$ 0.09)/μA ($R^2 = 0.9956$), demonstrating a wide linear response for the modified electrode. Due to saturation of electroactive sites, at higher concentration of CySH the sensitivity of the modified electrode is decreased.

Cyclic voltammograms of PBS containing CySH at different scan rates are recorded (not shown). The peak current for the anodic oxidation of CySH is proportional to the square root of the scan rate, suggesting that the process is controlled by diffusion of analyte as expected for a catalytic system. The relationship between the scan rate-normalized current ($I_p/\upsilon^{1/2}$) and the scan rate (υ) for CySH oxidation is investigated at GC/DNA/NiOx/Os(III)-complex modified electrode(Supplementary Fig. 4). The characteristic shape of a typical EC' catalytic process is obtained [58], suggesting that the reaction of CySH oxidation is controlled by an EC' mechanism. The Andriex and Saveant theoretical model [59] has been used to calculate the catalytic rate constant for an EC' mechanism. Based on this theory, the relationship between the peak current and the concentration of substrate for slow scan rates and large catalytic rate constant is as follows:

$$I_p = 0.446nFAD^{1/2}(\upsilon F/RT)^{1/2}C_s \quad (9)$$

Where D and C_s are the diffusion coefficient ($cm^2\ s^{-1}$) and the bulk concentration ($mol\ cm^{-3}$) of substrate (CySH), respectively and other symbols have their usual meanings. Low values of k_{cat} result in values of the coefficient (a) lower than 0.496. For low scan rates (5–20 mV s^{-1}), the average value of this coefficient was found to be 0.059. According to the Saveant approach and using Fig. 1 in Ref. [59] for a modified electrode with surface coverage of $3.2(\pm 0.1)\times 10^{-10}$ mol cm^{-2} for Os(III)-complex and a geometric area (A) of 0.085 cm^2, the average value of the calculated k_{cat} is 3.0 $(\pm 0.2)\times 10^3$ $M^{-1}\ s^{-1}$. High catalytic rate constant obtained for the Os(III)-complex further confirms its essential role as an efficient electron transfer mediator toward electrocatalytic oxidation of CySH.

3.4. Antifouling properties of the modified electrode

One of the major difficulties in the electrochemical methods for analysis of CySH is its high oxidation overpotentials at the conventional electrodes. So fouling of the electrode surface with the CySH oxidation products may be the major problem for determination of CySH [56,60]. In the present study, stability and antifouling properties of the modified electrode toward CySH oxidation are tested by measuring the decrease in the electrocatalytic oxidation current of CySH during successive potential cycling of the modified electrode. After 11 successive cyclic voltammograms of the modified electrode in 0.1 M PBS (pH 7) containing 1 mM CySH, no recognizable changes in peak current or peak potential of CysH have been observed (Fig. 5 of supplement), representing antifouling property of the nanocomposite modified electrode toward CySH and its oxidation products. The antifouling properties of GC/DNA/NiOx/Os(III)-complex electrode is one of the remarkable advantages of the proposed electrode toward CySH detection. In another test, the proposed nanocomposite modified electrode is stored in air in ambient condition and its response toward CySH oxidation is checked every day. After 30 days, the sensitivity of the modified electrode is measured as 94% of its initial value.

3.5. Amperometric detection of CySH

In order to investigate the effect of DNA/NiOx nanocomposite on the electrocatalytic oxidation of CySH, the typical amperometric responses of the different modified electrodes are examined. Fig. 7[A] exhibits the amperometric response of rotating GC/NiOxNPs/Os(III)-complex (a), GC/DNA/Os(III)-complex (b) and GC/DNA/NiOxNPs/Os(III)-complex (c) modified electrodes (rotation speed 600 rpm) for CySH oxidation at an applied potential of 0.1 V *vs.* Ag/AgCl in 0.1 M PBS (pH 7). It is clear that the GC/NiOx/Os(III)-complex electrode (amperogram "a") displays a very low current response after CySH addition. For GC/DNA/Os(III)-complex electrode (amperogram "b"), an unstable and weak current response is observed which was saturated after few additions, illustrating slight Os(III)-complex loading on the surface of GC/DNA modified electrode. However, for GC/DNA/NiOxNPs/Os(III)-complex electrode(amperogram"c"), a well-defined response is obtained after each addition of CySH, confirming high capacity of DNA/NiOx nanocomposite for Os(III)-complex loading. The calibration plots of catalytic currents vs. CySH concentration are shown in Fig. 7[B].

Fig. 8[A] displays the typical steady-state catalytic current–time response of the rotating modified electrode (2600 rpm) in PBS with successive injection of 1 μM of CySH at an applied potential of 0.10 V vs. Ag/AgCl. As can be seen, the modified electrode shows a rapid response, approaching 95% of the steady-state current within 3 s. The linear least square calibration graph over the range 1.0–11 μM (11 points) is $I/\mu A = 0.044\ (\pm\ 0.009)$[CySH]/μM + 0.0098 ($\pm$ 0.002)/μA with a correlation coefficient of 0.9993(Fig. 8B),

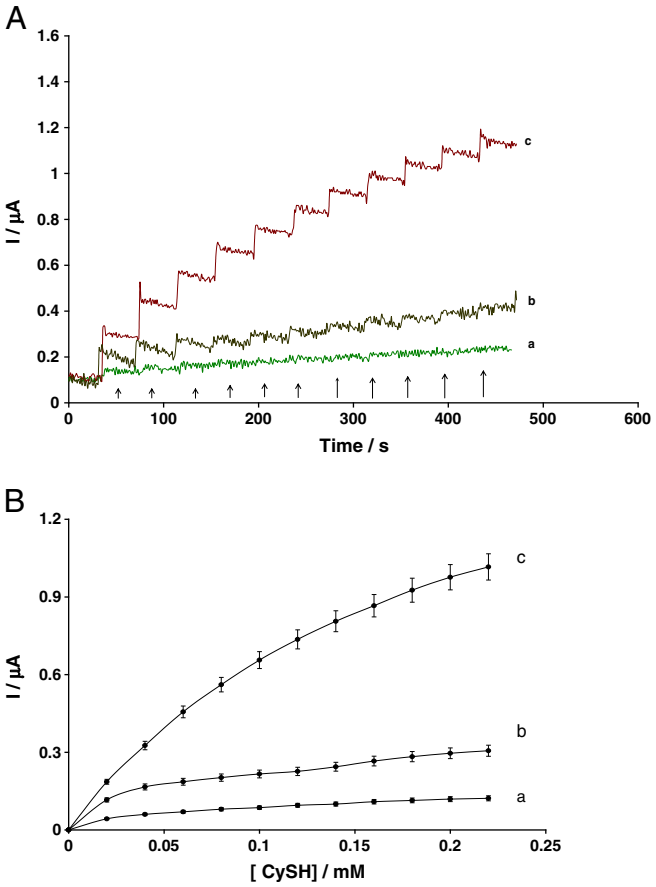

Fig. 7. (A) Amperometric response at the rotating GC/NiOxNPs/Os(III)-complex (a) GC/DNA/Os(III)-complex (b) and GC/DNA/NiOxNPs/Os(III)-complex (c) modified electrodes (rotation speed 600 rpm) in 0.1 M PBS (pH 7), applied potential 0.1 V *vs.* Ag/AgCl, for successive additions of 20 μM. (B) Plot of current response I/μA *vs.* concentration of cysteine [CySH/mM] for different modified electrodes.

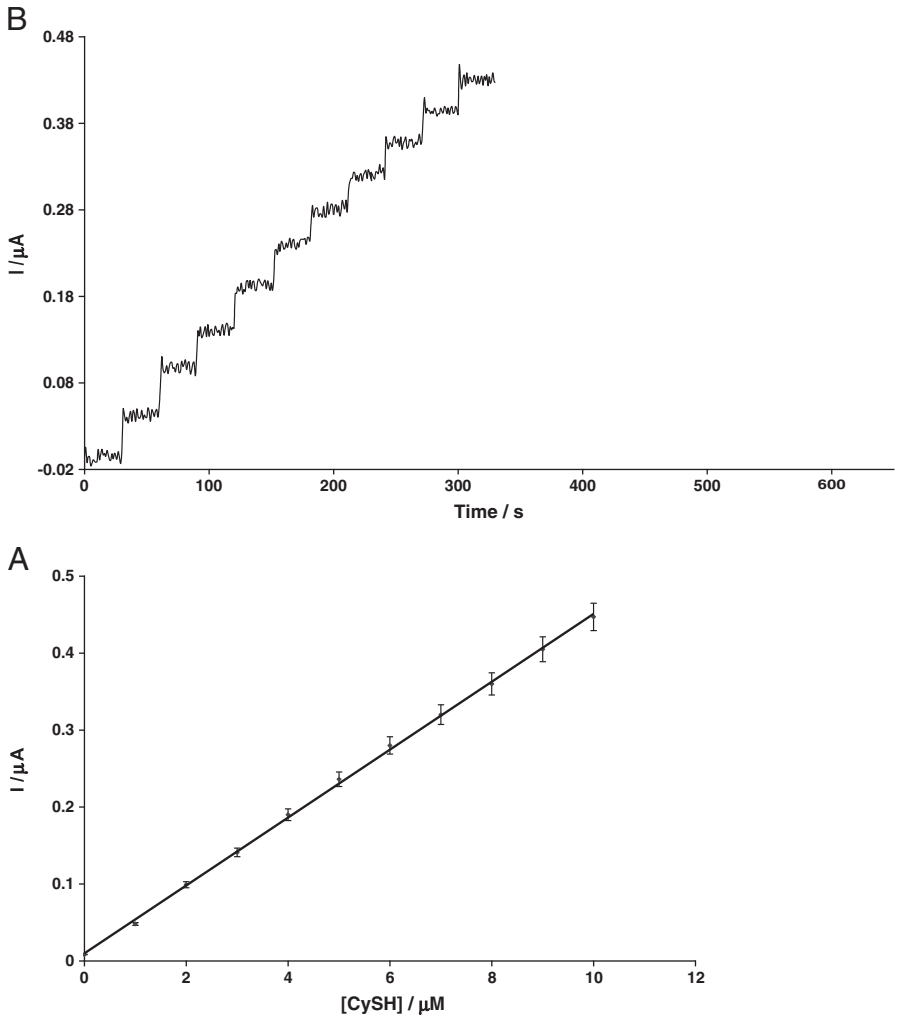

Fig. 8. (A) Amperometric response at the rotating GC/DNA/NiOxNPs/Os(III)-complex modified electrode (rotation speed 2600 rpm) in 0.1 M PBS (pH 7), applied potential 0.1 V *vs.* Ag/AgCl, for successive additions of 1 μM of CySH. (B) Plot of current response *I*/μA *vs*. concentration of cysteine [CySH/μM].

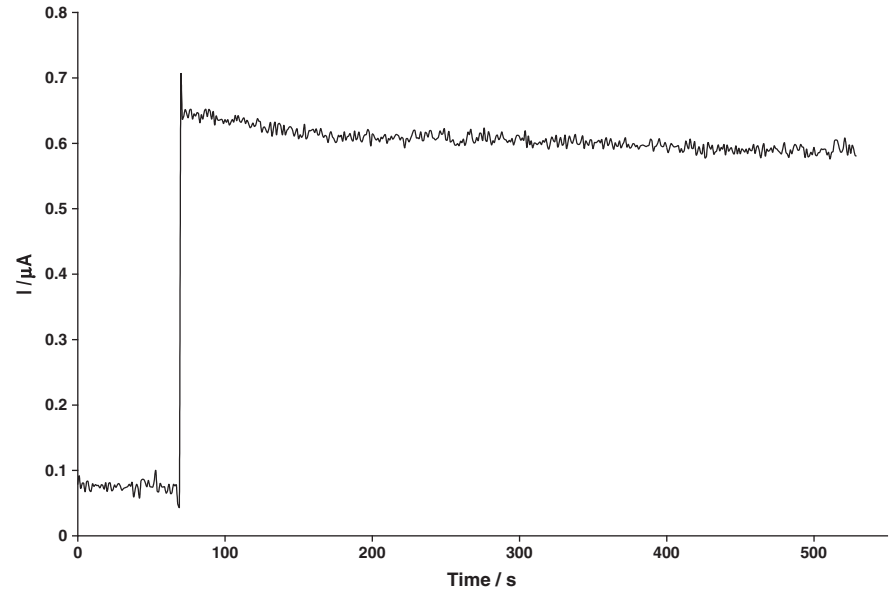

Fig. 9. Recorded chronoamperometric response at the rotating GC/DNA/NiOxNPs/Os(III)-complex modified electrode in 0.1 M PBS (pH 7) containing 20 μM CySH during 500 s. (rotation speed 2600 rpm and applied potential 0.1 V *vs.* Ag/AgCl).

indicating that the regression line is fitted very well with the experimental data and the regression equation can be applied in the unknown sample determination. The detection limit (based on signal to noise ratio of 3), sensitivity and linear concentration range of the sensor are obtained as 70 nM, 0.044 μA $\mu M^{-1,}$ and 1–1000 μM, respectively.

To improve the selectivity of CySH determination, the amperometric analysis of CySH is performed at an applied potential of 0.0 V *vs*. Ag/AgCl which showed a determination range of 3–400 μM and detection limit of 0.27 μM. Table 1 lists the response characteristics of the proposed CySH sensor in comparison to other reported CySH sensors in the literature. As it is obvious, the detection limit, sensitivity, linear concentration range and applied potential for the proposed sensor are comparable or better than the reported values for other electrochemical cysteine sensors.

The GC/DNA/NiOxNPs/Os(III)-complex electrode exhibits high stability onto amperometric measurements of CySH. Fig. 9 shows the amperometric response of 20 μM CySH recorded over a 500 s period. The result showed that the remaining percentage of initial response after 500 s is 95%, which demonstrates high stability of the modified electrode as well as absence of any inhibition effect of analyte or its oxidation products.

The operational stability of GC/DNA/NiOxNPs/Os(III)-complex electrode is assessed using 10 replicate amperometric measurements of 20 μM of CySH in PBS at an applied potential of 0.1 V and the relative standard deviation is calculated as 3.5%. Also, for 8 successive prepared electrodes, a relative standard deviation of 4% is obtained for measuring 20 μM of CySH. Furthermore, when the modified electrode is stored in the refrigerator at 4 °C, no significant change in the amperometric response for 20 μM of CySH is observed after 1 month. These results indicate good reproducibility, repeatability and stability of the modified electrode.

3.6. Selectivity of CySH detection

Selective detection of CySH in the presence of several interfering compounds potentially existing in biological liquids is a very advantageous feature for modified electrodes [34,61,62]. To demonstrate the selectivity of the proposed biosensor, the interferences of different compounds are examined during amperometric response for CySH. Fig. 10 shows the amperometric responses of GC/DNA/NiOxNPs/Os(III)-complex modified electrode toward CySH in the presence of some common oxidizable species found in biological fluids, such as homocysteine (HCySH), cystine, l-methionine, thiocytosine, glutathione, oxalic acid, dopamine, glucose and uric acid (applied potential = 0.0 V) in a 100 fold concentration of CySH. As can be found, no interfering effect is observed in the presence of 1 mM of each oxidizable compound. Thus, not only for low molecular-mass biothiols derivatives such as glutathione, L-cystine, L-methionine and electroactive biological species e.g. dopamine, uric acid and glucose, the electrocatalytic response is negligible but also for a very similar biothiol compound e.g. homocysteine (HCySH, which only difference between their molecular structures is one methylene–CH_2–), no recognizable response is observed on the modified electrode at the applied potential. The obtained results show the satisfactory selectivity of the proposed nanocomposite modified electrode toward electrooxidation of CySH at remarkable reduced overpotential. The results suggested that the coexistence of different interfering agents in the system does not affect the detection of CySH on GC/DNA/NiOxNPs/Os(III)-complex modified electrode. Therefore, the proposed electrode could be a practical sensor for determination of CySH in the mixture of various common oxidizable species without separation.

The selective interaction between DNA and CySH improves the sensor selectivity. The DNA/gold nanoparticles/Hg^{2+} and DNA/thiazole orange/Hg^{2+} systems were used for selective detection of CySH using fluorometric technique [63,64]. However, the interference effect of ascorbic acid is a major limitation of proposed GC/DNA/NiOxNPs/Os(III)-complex modified electrode. The AA signal can be suppressed by covering the modified electrode surface with a thin layer of nafion film. However, for GC/DNA/NiOxNPs/Os(III)-complex/nafion modified electrode the electrochemical response toward CySH oxidation slightly decreased (8%).

Table 2
Cysteine detection in serum samples.

	Cysteine added (μM)	Cysteine founded (μM), ($n=3$)	Recovery(%)
Blood serum	–	210.5(±4.0)	–
Blood serum	20.0	228.0 (±5.0)	98.9 (±2.0)
Blood serum	50.0	258.0 (±5.0)	99. 0(±2.0)
Blood serum	–	195.50	–
Blood serum	30	223.70(±5.0)	99.0 (±2.0)
Blood serum	60	257.50(±4.0)	100.7(±2.0)
Blood serum	90	282.60(±5.0)	98.9(±1.5)

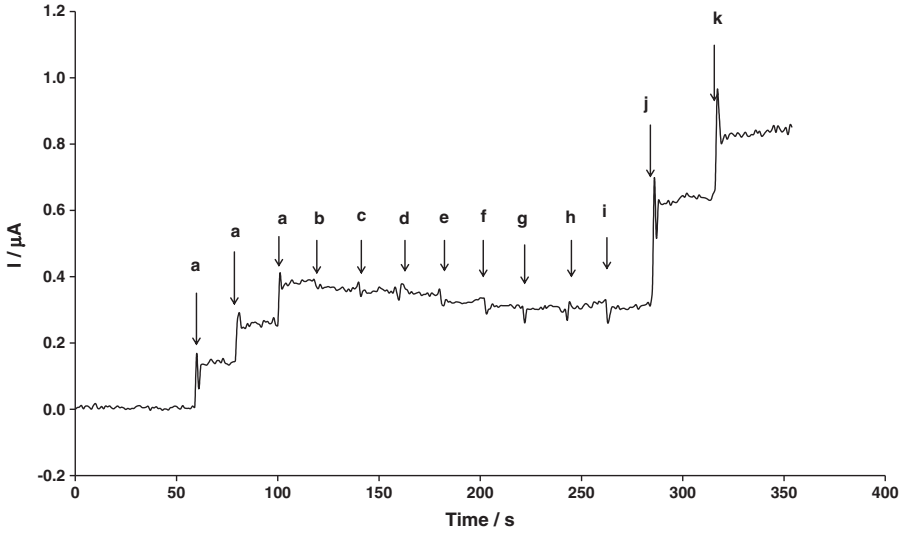

Fig. 10. Current responses obtained at the GC/DNA/NiOxNPs/Os(III)-complex modified electrode in 0.1 M PBS (pH 7) for the additions (indicated by arrows) of 10 μM of CySH (a) and 0.1 mM of L-methionine (b), glutathione (c), oxalic acid (d), dopamine (e), uric acid (f), HCySH (g), thiocytosine (h),cystine (i) and 20 μM CySH(j, k). (Applied potential: 0.0 V *vs.* Ag/AgCl , rotation speed 2600 rpm).

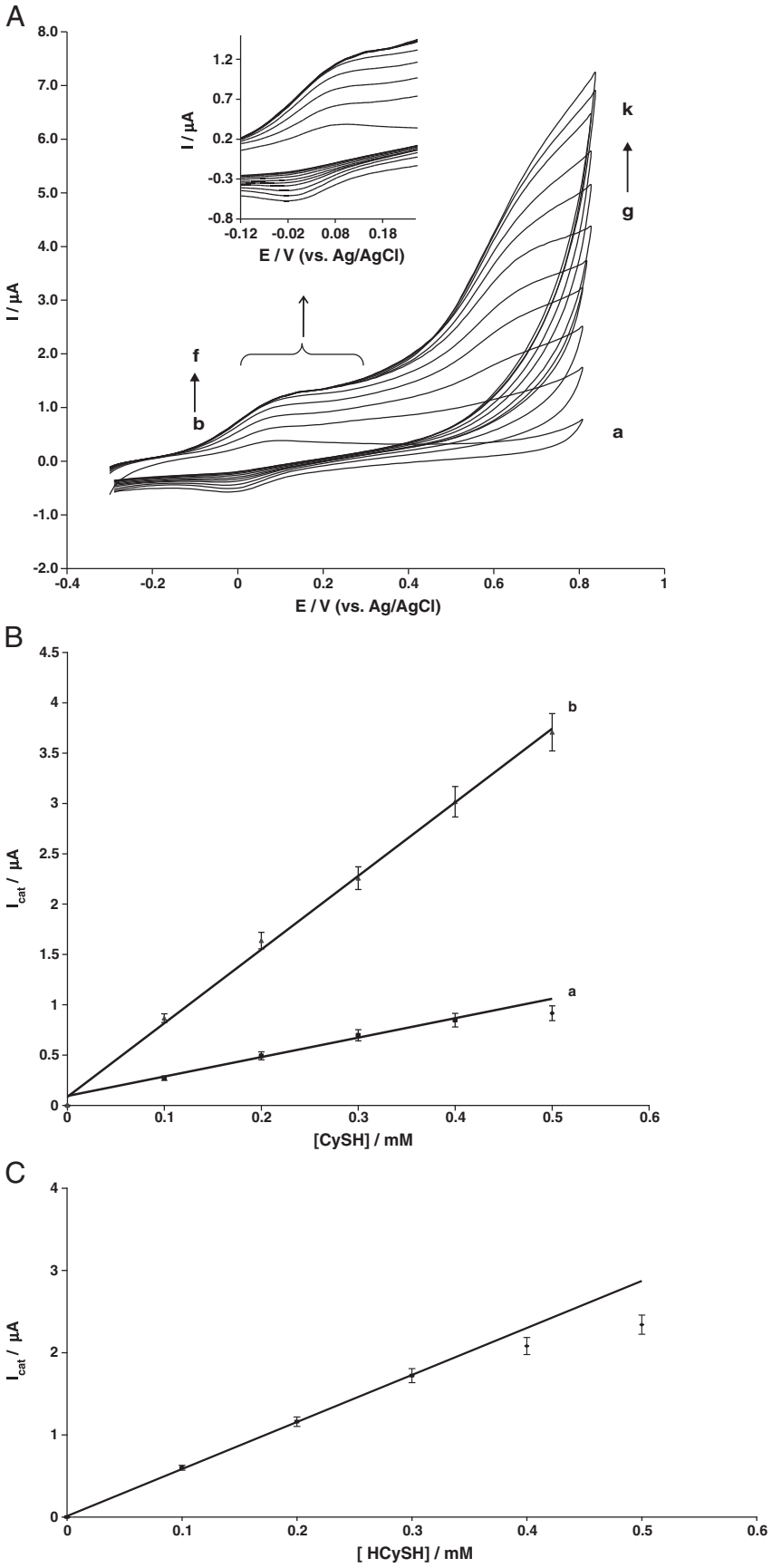

Fig. 11. (A) Cyclic voltammograms of GC/DNA/NiOxNPs/Os(III)-complex modified electrode (a) in 0.1 M PBS (pH 7) (b to f) as (a) in the presence of various concentration of CySH (0.1, 0.2, 0.3, 0.4, 0.5/mM) and (g to f) as (b to f), with increasing different concentrations of HCySH (0.1, 0.2, 0.3, 0.4, 0.5/mM) at scan rate 20 mV s^{-1}.(B) Plot of catalytic peak current I_p/µA *vs.* concentration of cysteine [CySH/mM], (a) first peak oxidation current and (b) second peak oxidation current. (C) Plot of catalytic peak current I_p/µA *vs.* concentration of homocysteine [HCySH/mM].

3.7. Determination of cysteine in real samples

The applicability of the proposed biosensor for CySH determination in serum samples is investigated and results are presented in Table 2. Due to interference of AA, the modified electrode covered with a thin film of nafion is used for CySH detection in real samples. The standard addition method is adopted for CySH detection in real sample and a calibration curve was obtained for each sample. The concentration of CySH in serum sample is found to be 195.5–210.5 μM, which is a normal dosage for CySH in serum samples [65,66]. To confirm the validity of the results, the serum samples are spiked with defined amount of CySH at levels similar to those found in the samples. The obtained results in Table 2 demonstrate satisfactory recoveries, varying between 95% and 102% for spiked CySH. Therefore, the modified proposed sensor can be used for CySH detection in real samples.

3.8. Simultaneous detection of cysteine and homocysteine

The possibility of simultaneous determination of CySH and HCySH was investigated on different modified electrodes of GC/NiOxNPs, GC/DNA, GC/DNA/NiOxNPs and GC/DNA/NiOxNPs/Os(III)-complex. The voltammetric peaks of HCySH and CySH for first three modified electrodes are completely overlapped (data not shown). However, because of the different oxidation potentials of these two compounds on the GC/DNA/NiOxNPs/Os(III)-complex modified electrode, the simultaneous voltammetric detection of CySH and HCySH without requiring separation process is possible. The electrocatalytic oxidation of both CySH and HCySH occurred at GC/DNA/NiOxNPs/Os(III)-complex modified electrode. Selective interaction between DNA and CySH improves the sensor selectivity, and oxidation peak potential for proposed analytes observed at different potentials. Fig. 11 [A] shows typical cyclic voltammograms obtained for mixture solutions containing various concentrations of CySH and HCySH. As can be seen, with increasing CySH concentration, the observed anodic peaks current at +0.10 V and +0.65 V increased (curves b–f). Interestingly, with injection of HCySH to buffer solution containing CySH, no recognizable change is observed for the anodic peak current of CySH at 0.1 V(inset of Fig. 11), while the anodic response of HCySH at 0.6 V increased proportionally with increasing HCySH concentration (curves g–k). Fig. 11 [B] shows the calibration curves for CySH using the anodic peak currents of CySH at (a) 0.1 V and (b) 0.6 V. The regression equations over the applied potentials are I (μA) = 1.93 (± 0.05) [CySH]/(mM) + 0.093 (± 0.003)/ μA (R^2 = 0.9928) and I (μA) = 7.315 (±0.11) [CySH]/(mM) + 0.085(± 0.004)/μA (R^2 = 0.9979), respectively. Concentration of CySH is determined using its first calibration curve. According to the second calibration curve of CySH, the current's portion of HCySH in the second peak is estimated. The cyclic voltammograms of the modified electrode in 0.1 M PBS, in the presence of constant value (0.4 mM) of CySH and various amounts of HCySH are investigated (voltammograms g–k). The plotted calibration curve for HCySH in concentration range of 0.1 mM–1.2 mM is obtained with a regression equation of: I (μA) = 5.72(± 0.08) [HCySH]/(mM) + 0.012 (± 0.001)/μA (R^2 = 0.9997) (Fig. 11 [C]). The cyclic voltammograms of modified electrode in the presence fixed concentration of HCySH (0.1 mM) and various concentrations of CySH are recorded (Fig. 6 Supplement). The plotted calibration curve for CySH in concentration range of 0.1 mM–0.5 mM is obtained with a regression equations of: I (μA) = 2.29 (± 0.06) [CySH]/(mM)–0.021 (± 0.006)/μA (R^2 = 0.9972) for the first pea and I (μA) = 15.62 (±0.16) [CySH]/(mM) + 0.23 (± 0.01)/μA (R^2 = 0.9979 for the second peak respectively. The hydrodynamic amperometry technique is promised for HCySH detection at micromolar or lower concentration range.

4. Conclusions

The development of a new CySH sensor was reported based on GC/DNA/NiOx/ Os(III)-complex modified electrode with some desirable characteristics, such as wide linear range, low detection limit and a long-term stability. The results indicated that the DNA/NiOx/Os(III)-complex film provided a well-defined peak-shaped response for the CysH oxidation at lower oxidation potential compared to the previously reported electrodes. High selectivity, excellent electrocatalytic activity, remarkable antifouling property toward thiols and their oxidation products as well as the ability for simultaneous detection of L-cysteine and homocysteine are other remarkable advantages of the proposed biosensor. Due to its excellent resistance to surface fouling and its renewable surface, the electrode was successfully applied for direct analysis of CySH in real samples containing various oxidizable species.

Acknowledgments

This research was supported by the Iranian Nanotechnology Initiative and the Research Offices of the University of Kurdistan and Isfahan University.

Appendix A. Supplementary data

Supplementary data to this article can be found online at doi:10.1016/j.bioelechem.2011.12.013.

References

[1] M. Hung, D.M. Stanbury, Catalytic and direct oxidation of cysteine by octacyanomolybdate(V), Inorg. Chem. 44 (2005) 3541–3550.
[2] T. Inoue, J.R. Kirchhoff, Electrochemical detection of thiols with a coenzyme pyrroloquinoline quinone modified electrode, Anal. Chem. 72 (2000) 5755–5760.
[3] M.M. Ardakani, P. Rahimi, P.E. Karami, H.R. Zare, H. Naeimi, Electrocatalytic oxidation of cysteine by quinizarine at glassy carbon electrode, Sens. Actuators, B 123 (2007) 763–768.
[4] S. Shahrokhian, Lead phthalocyanine as a selective carrier for preparation of a cysteine-selective electrode, Anal. Chem. 73 (2001) 5972–5978.
[5] P.C. White, N.S. Lawrence, J. Davis, R.G. Compton, Electrochemically initiated 1,4 additions: a versatile route to the determination of thiols, Anal. Chim. Acta 447 (2001) 1–10.
[6] S. Seshadri, A. Beiser, J. Selhub, P.F. Jacques, I.H. Rosenberg, R.B. D'Agostino, P.W.F.N. Wilson, Plasma homocysteine as a risk factor for dementia and Alzheimer's disease, N Engl J. Med. 346 (2002) 476–483.
[7] M.A. Hofmann, B. Kohl, M.S. Zumbach, V. Borcea, A. Bierhaus, M. Henkels, J. Amiral, W. Fiehn, R. Ziegler, P. Wahl, P.P. Nawroth, Hyperhomocyst(e)inemia and endothelial dysfunction in IDDM, Diabetes Care 20 (1997) 1880–1886.
[8] E.K. Hoogeveen, P.J. Kostense, P.J. Beks, C. Jakobs, L.M. Bouter, R.J. Heine, C.D. Stehouwer, Hyperhomocysteinemia is associated with an increased risk of cardiovascular disease, especially in non-insulin-dependent diabetes mellitus, Arterioscler. Thromb. Vasc. Biol. 18 (1998) 133–138.
[9] B. Hultberg, E. Agargh, A. Andersson, L. Brattstrom, A. Isaksson, B. Israelsson, C.D. Agardh, J. increased leveles of plasma homocysteine are associated with nephropathy, but not severe retinopathy in type I diabetes mellitus, Scand. Clin. Lab. Invest. 51 (1991) 277–282.
[10] A. Splaver, G.A. Lamas, C.H. Hennekens, Homocysteine and cardiovascular disease: biological mechanisms, observational epidemiology, and the need for randomized trials, Am. Heart J. 148 (2004) 34–40.
[11] W. Wang, O. Rusin, X. Xu, K.K. Kim, J.O. Escobedo, S.O. Fakayode, K.A. Fletcher, M. Lowry, C.M. Schowalter, C.M. Lawrence, F.R. Fronczek, I.M. Warner, R.M. Strongin, Detection of homocysteine and cysteine, J. Am. Chem. Soc. 127 (2005) 15949–15958.
[12] R. Zhang, X. Yu, Z. Ye, G. Wang, W. Zhang, J. Yuan, Turn-on luminescent probe for cysteine/homocysteine based on a ruthenium(II) complex, Inorg. Chem. 49 (2010) 7898–7903.
[13] H. Refsum, A.D. Smith, P.M. Ueland, E. Nexo, R. Clarke, J. McPartlin, C. Johnston, F. Engbaek, J. Schneede, C. McPartlin, J.M. Scott, Facts and recommendations about total homocysteine determinations: an expert opinion, Clin. Chem. 50 (2004) 3–32.
[14] O. Rusin, N.N. St. Luce, R.A. Agbaria, J.O. Escobedo, S. Jiang, I.M. Warner, F.B. Dawan, K. Lian, R.M. Strongin, Visual detection of cysteine and homocysteine, J. Am. Chem. Soc. 126 (2004) 438–439.
[15] G. Chwatko, E. Bald, Determination of cysteine in human plasma by high-performance liquid chromatography and ultraviolet detection after pre-column derivatization with 2-chloro-1-methylpyridinium iodide, Talanta 52 (2000) 509–515.

[16] A. Sano, H. Nakamure, Chemiluminescence detection of thiols by high-performance liquid chromatography using o-phthalaldehyde and N-(4-aminobutyl)-N-ethylisoluminol as precolumn derivatization reagents, Anal. Sci. 14 (1998) 731–737.
[17] K. Arlt, S. Brandt, J. Kehr, Amino acid analysis in five pooled single plant cell samples using capillary electrophoresis coupled to laser-induced fluorescence detection, J. Chromatogr. A 926 (2001) 319–325.
[18] M. Ummadi, B.C. Weimer, Use of capillary electrophoresis and laser-induced fluorescence for attomole detection of amino acids, J. Chromatogr. A 964 (2002) 243–253.
[19] F. Tanaka, N. Mase, C.F. Barbas III, Determination of cysteine concentration by fluorescence increase: reaction of cysteine with a fluorogenic aldehyde, Chem. Commun. (2004) 1762–1763.
[20] D.A.M. Zaia, K.C.L. Ribas, C.T.B.V. Zaia, Spectrophotometric determination of cysteine and/or carbocysteine in a mixture of amino acids, shampoo, and pharmaceutical products using p-benzoquinone, Talanta 50 (1999) 1003–1010.
[21] G. Shi, J. Lu, F. Xu, W. Sun, L. Jin, K. Yamamoto, S. Tao, J. Jin, Determination of glutathione in vivo by microdialysis using liquid chromatography with a cobalt hexacyanoferrate chemically modified electrode, Anal. Chim. Acta 391 (1999) 307–313.
[22] X. Chen, B. Xia, P. He, Dynamics of the electrocatalytic oxidation of cysteine at nafion film coated electrodes, J. Electroanal. Chem. Interfacial Electrochem. 281 (1990) 185–198.
[23] W.R. Fawcett, M. Fedurco, Z. Kovácová, Z. Borkowska, Oxidation of cysteine, cysteinesulfinic acid and cysteic acid on a polycrystalline gold electrode, J. Electroanal. Chem. 368 (1994) 265–274.
[24] M.K. Halbert, R.P. Baldwin, Electrocatalytic and analytical response of cobalt phthalocyanine containing carbon paste electrodes toward sulfhydryl compounds, Anal. Chem. 57 (1985) 591–595.
[25] J. Koryta, J. Pradác, Electrode processes of the sulfhydryl-disulfide system III. cysteine at platinum and gold electrodes, J. Electroanal. Chem. 17 (1968) 185–189.
[26] E.F. Perez, L.T. Kubota, A.A. Tanaka, G. De Oliveira Neto, Anodic oxidation of cysteine catalysed by nickel tetrasulphonated phthalocyanine immobilized on silica gel modified with titanium (IV) oxide, Electrochim. Acta 43 (1998) 1665–1673.
[27] M.K. Amini, J.H. Khorasani, S.S. Khaloo, S. Tangestaninejad, Cobalt(II) salophen-modified carbon-paste electrode for potentiometric and voltammetric determination of cysteine, Anal. Biochem. 320 (2003) 32–38.
[28] X. Tang, Y. Liu, H. Hou, T. You, Electrochemical determination of L-tryptophan, L-tyrosine and L-cysteine using electrospun carbon nanofibers modified electrode, Talanta 80 (2010) 2182–2186.
[29] P. Lochman, T. Adam, D. Friedecký, E. Hlídková, Z. Škopková, High-throughput capillary electrophoretic method for determination of total aminothiols in plasma and urine, Electrophoresis 24 (2003) 1200–1207.
[30] A. Pastore, R. Massoud, C. Motti, A.L. Russo, G. Fucci, C. Cortese, G. Federici, Fully automated assay for total homocysteine, cysteine, cysteinylglycine, glutathione, cysteamine, and 2-mercaptopropionylglycine in plasma and urine, Clin. Chem. 44 (1998) 825–832.
[31] T. Inoue, J.R. Kirchhoff, Determination of thiols by capillary electrophoresis with amperometric detection at a coenzyme pyrroloquinoline quinone modified electrode, Anal. Chem. 74 (2002) 1349–1354.
[32] S.A. Pasas, N.A. Lacher, M.I. Davies, S.M. Lunte, Detection of homocysteine by conventional and microchip capillary electrophoresis/electrochemistry, Electrophoresis 23 (2002) 759–766.
[33] M. Zhong, S.M. Lunte, Tubular-wire dual electrode for detection of thiols and disulfides by capillary electrophoresis/electrochemistry, Anal. Chem. 71 (1999) 251–255.
[34] Z. Chen, Y. Zu, Electrochemical recognition of single-methylene difference between cysteine and homocysteine, J. Electroanal. Chem. 624 (2008) 9–13.
[35] C.L. Carnes, K.J. Klabunde, The catalytic methanol synthesis over nanoparticle metal oxide catalysts, J. Mol. Catal. A: Chem. 194 (2003) 227–236.
[36] Y. Ichiyanagi, N. Wakabayashi, J. Yamazaki, S. Yamada, Y. Kimishima, E. Komatsu, H. Tajima, Magnetic properties of NiO nanoparticles, Physica B 862 (2003) 329–333.
[37] A. Noorbakhsh, A. Salimi, Amperometric detection of hydrogen peroxide at nano-nickel oxide/thionine and celestine blue nanocomposite-modified glassy carbon electrodes, Electrochim. Acta 54 (2009) 6312–6321.
[38] A. Salimi, E. Sharifi, A. Noorbakhsh, S. Soltanian, Direct voltammetry and electrocatalytic properties of hemoglobin immobilized on a glassy carbon electrode modified with nickel oxide nanoparticles, Electrochem. Commun. 8 (2006) 1499–1508.
[39] A. Salimi, E. Sharifi, A. Noorbakhsh, S. Soltanian, Immobilization of glucose oxidase on electrodeposited nickel oxide nanoparticles: direct electron transfer and electrocatalytic activity, Biosens. Bioelectron. 22 (2007) 3146–3153.
[40] E.M. Boon, N.M. Jackson, M.D. Wightman, S.O. Kelley, M.G. Hill, J.K. Barton, Intercalative stacking: a critical feature of DNA charge-transport electrochemistry, J. Phys. Chem. B 107 (2003) 11805–11812.
[41] D. Ly, L. Sanii, G.B. Schuster, Mechanism of charge transport in DNA: internally-linked anthraquinone conjugates support phonon-assisted polaron hopping, J. Am. Chem. Soc. 121 (1999) 9400–9410.
[42] Y. Okahata, T. Kobayashi, K. Tanaka, M. Shimomura, Anisotropic electric conductivity in an aligned DNA cast film, J. Am. Chem. Soc. 120 (1998) 6165–6166.
[43] T. Rajh, Z. Saponjic, J. Liu, N.M. Dimitrijevic, N.F. Scherer, M. Vega-Arroyo, P. Zapol, L.A. Curtiss, M.C. Thurnauer, Charge transfer across the nanocrystalline–DNA interface: probing DNA recognition, Nano Lett. 4 (2004) 1017–1023.
[44] Z. Chen, H. Zheng, C. Lu, Y. Zu, Oxidation of L-cysteine at a fluorosurfactant-modified gold electrode: lower overpotential and higher selectivity, Langmuir 23 (2007) 10816–10822.
[45] J.L. Chávez, W. Lyon, N. Kelley-Loughnane, M.O. Stone, Theophylline detection using an aptamer and DNA-gold nanoparticle conjugates, Biosens. Bioelectron. 26 (2010) 23–28.
[46] J.A. Ribeiro, C.A. Carreira, H.J. Lee, F. Silva, A. Martins, C.M. Pereira, Voltammetric determination of paraquat at DNA-gold nanoparticle composite electrodes, Electrochim. Acta 55 (2010) 7892–7896.
[47] P.-H. Lo, S.A. Kumar, S.-M. Chen, Amperometric determination of H_2O_2 at nano-TiO_2/DNA/thionin nanocomposite modified electrode, Colloids Surf. B Biointerfaces 66 (2008) 266–273.
[48] J.J. Storhoff, C.A. Mirkin, Programmed materials synthesis with DNA, Chem. Rev. 99 (1999) 1849–1862.
[49] Z. Liu, Y. Zu, Y. Fu, Y. Zhang, H. Liang, Growth of the oxidized nickel nanoparticles on a DNA template in aqueous solution, Mater. Lett. 62 (2008) 2315–2317.
[50] C.M. Che, W.K. Cheng, T.F. Lai, C.K. Poon, T.C.W. Mak, Stabilization of high-valent transition-metal complexes with macrocyclic tertiary amines. Reinvestigation of the synthesis, electrochemistry, and spectroscopy of osmium(III) macrocyclic amine complexes and x-ray crystal structure of trans-[OsIII(16-TMC)Cl_2]ClO_4 (16-TMC = 1,5,9,13-tetramethyl-1,5,9,13-tetraazacyclohexadecane), Inorg. Chem. 26 (1987) 1678–1683.
[51] X. Lin, X. Jiang, L. Lu, DNA deposition on carbon electrodes under controlled dc potentials, Biosens. Bioelectron. 20 (2005) 1709–1717.
[52] D. Giovanelli, N.S. Lawrence, L. Jiang, T.G.J. Jones, R.G. Compton, Electrochemical determination of sulphide at nickel electrodes in alkaline media: a new electrochemical sensor, Sens. Actuators, B 88 (2003) 320–328.
[53] A. Salimi, B. Kavosi, A. Babaei, R. Hallaj, Electrosorption of Os(III)-complex at single-wall carbon nanotubes immobilized on a glassy carbon electrode: application to nanomolar detection of bromate, periodate and iodate, Anal. Chim. Acta 618 (2008) 43–53.
[54] E. Laviron, Adsorption, autoinhibition and autocatalysis in polarography and in linear potential sweep voltammetry, J. Electroanal. Chem. 52 (1974) 355–393.
[55] X.-B. Yin, Y.-Y. Xin, Y. Zhao, Label-free electrochemiluminescent aptasensor with attomolar mass detection limits based on a Ru$(phen)_3^{2+}$-double-strand DNA composite film electrode, Anal. Chem. 81 (2009) 9299–9305.
[56] T.R. Ralph, M.L. Hitchman, J.P. Millington, F.C. Walsh, The electrochemistry of l-cystine and l-cysteine: Part 1: thermodynamic and kinetic studies, J. Electroanal. Chem. 375 (1994) 1–15.
[57] M. Zhou, J. Ding, L.-p. Guo, Q.-k. Shang, Electrochemical behavior of L-cysteine and its detection at ordered mesoporous carbon-modified glassy carbon electrode, Anal. Chem. 79 (2007) 5328–5335.
[58] F. Pariente, E. Lorenzo, F. Tobalina, H.D. Abruna, Aldehyde biosensor based on the determination of NADH enzymically generated by aldehyde dehydrogenase, Anal. Chem. 67 (1995) 3936–3944.
[59] C.P. Andrieux, J.M. Saveant, Heterogeneous (chemically modified electrodes, polymer electrodes) vs. homogeneous catalysis of electrochemical reactions, J. Electroanal. Chem. Interfacial Electrochem. 93 (1978) 163–168.
[60] N. Maleki, A. Safavi, F. Sedaghati, F. Tajabadi, Efficient electrocatalysis of L-cysteine oxidation at carbon ionic liquid electrode, Anal. Biochem. 369 (2007) 149–153.
[61] Y.-H. Bai, J.-J. Xu, H.-Y. Chen, Selective sensing of cysteine on manganese dioxide nanowires and chitosan modified glassy carbon electrodes, Biosens. Bioelectron. 24 (2009) 2985–2990.
[62] G. Chen, J. Zhao, X. Liu, G. Gao, J. Huang, G. Li, Electrochemical sensing DNA damage with nano-titanium dioxide and repair with a medicinal herb species resveratrol, J. Biotechnol. 127 (2007) 653–656.
[63] F. Pu, Z. Huang, J. Ren, X. Qu, DNA/ligand/ion-based ensemble for fluorescence turn on detection of cysteine and histidine with tunable dynamic range, Anal. Chem. 82 (2010) 8211–8216.
[64] J.-S. Lee, P.A. Ulmann, M.S. Han, C.A. Mirkin, A DNA-gold nanoparticle-based colorimetric competition assay for the detection of cysteine, Nano Lett. 8 (2008) 529–533.
[65] A.A. Ensafi, S. Behyan, Sensing of L-cysteine at glassy carbon electrode using Nile blue A as a mediator, Sens. Actuators, B 122 (2007) 282–288.
[66] S.P. Stabler, P.D. Marcell, E.R. Podell, R.H. Allen, Quantitation of total homocysteine, total cysteine, and methionine in normal serum and urine using capillary gas chromatography–mass spectrometry, Anal. Biochem. 162 (1987) 185–196.
[67] R. Ojani, J.-B. Raoof, E. Zarei, Preparation of poly *N*,*N*-dimethylaniline/ferrocyanide film modified carbon paste electrode: application to electrocatalytic oxidation of l-cysteine, J. Electroanal. Chem. 638 (2010) 241–245.
[68] J.C. Ndamanisha, J. Bai, B. Qi, L. Guo, Application of electrochemical properties of ordered mesoporous carbon to the determination of glutathione and cysteine, Anal. Biochem. 386 (2009) 79–84.
[69] C. Deng, J. Chen, X. Chen, M. Wang, Z. Nie, S. Yao, Electrochemical detection of l-cysteine using a boron-doped carbon nanotube-modified electrode, Electrochim. Acta 54 (2009) 3298–3302.
[70] R. Hallaj, A. Salimi, K. Akhtari, S. Soltanian, H. Mamkhezri, Electrodeposition of guanine oxidation product onto zinc oxide nanoparticles: application to nanomolar detection of L-cysteine, Sens. Actuators, B 135 (2009) 632–641.
[71] A. Abbaspour, A. Ghaffarinejad, Electrocatalytic oxidation of L-cysteine with a stable copper-cobalt hexacyanoferrate electrochemically modified carbon paste electrode, Electrochim. Acta 53 (2008) 6643–6650.
[72] W.-Y. Su, S.-H. Cheng, Electrocatalysis and sensitive determination of cysteine at poly(3,4-ethylenedioxythiophene)-modified screen-printed electrodes, Electrochem. Commun. 10 (2008) 899–902.
[73] X. Chen, Y. Yang, M. Ding, Electrocatalytic oxidation and sensitive detection of cysteine at layer-by-layer assembled carbon nanotube-modified electrode, Anal. Chim. Acta 557 (2006) 52–56.
[74] A. Salimi, R. Hallaj, Catalytic oxidation of thiols at preheated glassy carbon electrode modified with abrasive immobilization of multiwall carbon nanotubes:

applications to amperometric detection of thiocytosine, L-cysteine and glutathione, Talanta 66 (2005) 967–975.
[75] S. Fei, J. Chen, S. Yao, G. Deng, D. He, Y. Kuang, Electrochemical behavior of L-cysteine and its detection at carbon nanotube electrode modified with platinum, Anal. Biochem. 339 (2005) 29–35.
[76] A. Salimi, S. Pourbeyram, Renewable sol–gel carbon ceramic electrodes modified with a Ru-complex for the amperometric detection of -cysteine and glutathione, Talanta 60 (2003) 205–214.
[77] J.-M. Zen, A.S. Kumar, J.-C. Chen, Electrocatalytic oxidation and sensitive detection of cysteine on a lead ruthenate pyrochlore modified electrode, Anal. Chem. 73 (2001) 1169–1175.

Ensiyeh Sharifi. received the BS degree in Chemistry from Shiraz University, Shiraz, Iran, in 2003; completed his MSc in February 2007 in University of Kurdistan, Sanandaj, Iran. Now she is a PhD student in Isfahan University. Her research work has been mainly focused on fabrication of new sensor and biosensors based on DNA, metal oxide nanoparticles, quantum dot and different organic and organometalic electron transfer mediators.

Abdollah Salimi. graduated in analytical chemistry in 1994 from Tabriz University, Iran. Since the same year he joined the department of chemistry at University of Kurdistan (Sanandaj-Iran). During 1995–1999 he completed his PhD at the Tarbiat Modaress University (Tehran-Iran) in electrochemistry. Currently he is working as professor in University of Kurdistan, Sanandaj, Iran. His current research interests are novel nanomaterials based sensors and biosensors, DNA hybridization, aptamer based electrochemical sensors, nanobioelectrochemistry and electron transfer kinetics.

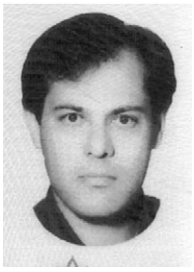

Esmaeil Shams Solari. is an associate professor of Analytical Chemistry at Isfahan University, Isfahan, Iran. He received the BS degree in chemistry from Isfahan University, in 1992, and the MS degree from Isfahan University of Technology (IUT), Iran, in 1994. In 1998, he received his Ph.D. degree in analytical chemistry from the University of Shiraz, Shiraz, Iran. From January 1998 to May 2005 he worked at the Institute for Advanced Studies in Basic Sciences, Zanjan, Iran. Since June 2005 he has joined the department of chemistry at the Isfahan University. His current researches are focused on the development of adsorptive stripping voltammetric methods for the determination of heavy metals and development of electrochemical sensors based on chemically modified electrodes.